

Low-Sidelobe Design of Intelligent Reflecting Surface Using Liquid Chrystal

1st Hiroyasu Sato

Department of Communications Engineering,
Graduate School of Engineering, Tohoku University
Sendai, Japan
hiroyasu.sato.b1@tohoku.ac.jp

3th Hideo Fujikake

Department of Communications Engineering,
Graduate School of Engineering, Tohoku University
Sendai, Japan
hideo.fujikake.e6@tohoku.ac.jp

2nd Rio Matsuda

Department of Communications Engineering,
Graduate School of Engineering, Tohoku University
Sendai, Japan
rio.matsuda.q6@tohoku.ac.jp

4th Qiang Chen

Department of Communications Engineering,
Graduate School of Engineering, Tohoku University
Sendai, Japan
qiang.chen.a5@tohoku.ac.jp

Abstract—In this paper, low sidelobe design of Liquid Crystal-based Intelligent Reflecting Surface at 47 GHz band has been demonstrated. It is found that both the large phase change of over 360 degrees, the constant reflection magnitude change is important to obtain low sidelobe scattering pattern used for IRS applications such as 5G communications.

Keywords—IRS, Liquid Crystal, Scattering, Sidelobe level

I. INTRODUCTION

In Intelligent Reflecting surface (IRS) technology for 5G communications, which electrically controls the direction of reflection, has been attracting attention in recent years. Among the IRS using diodes or MEMS are being researched as a typical phase control technology for realizing IRS, the liquid crystal-based IRS (LC-IRS) is also expected for 5G and 6G communications based on the liquid crystal display technology. The phase is changed by controlling the dielectric constant of LCs to actively scanning the direction of the reflected beam.

When a voltage is applied to the liquid crystal, permittivity of the liquid crystal slightly changes (typically 2.5 - 3), and this change is used to change the effective length of each reflectarray elements and to change the reflection phase. Although the LC-IRS has the advantage of being able to achieve continuous phase, which is difficult to achieve with 1-bit or 2-bit reflect arrays, it has the disadvantage that the magnitude of the reflection coefficient also changes.

In this paper, we propose a method to reduce the change of the reflection magnitude by lowering the Q-value of the resonance of printed dipoles. Also a scattering pattern with low sidelobes is demonstrated by the array factor analysis.

II. DESIGN OF UNIT CELL

Figure 1 shows a photograph of the LC-IRS and the structure of the unit cell with pitch p . The design frequency is set to 47 GHz band. Developed liquid crystal of TD-1020XX [1, 2] was used. Model A consists of three dipoles, the length of the central element is l_1 , the upper and lower elements are l_2 , and the width of each dipole is w . Model B consists of two dipoles with the length and width of l_1 , w_1 and l_2 , w_2 , respectively. These conducting structures are etched onto an alkali-free glass substrate with a thickness of h_1 and used to seal the liquid crystal with a thickness of the liquid crystal

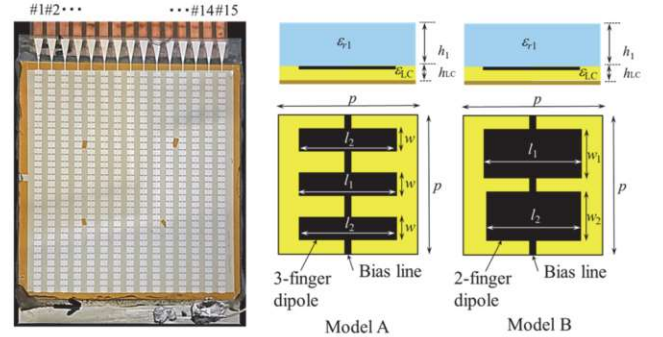


Figure 1. Photograph of Liquid Crystal-based Intelligent Reflect Surface and structure of unit cell (Model A, Model B).

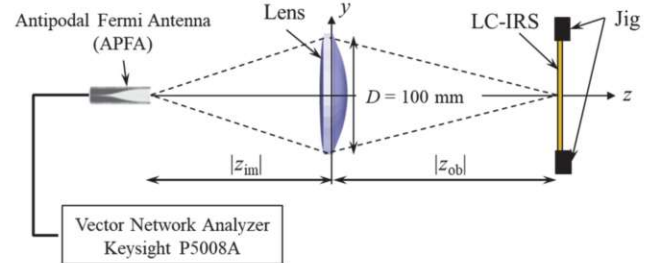


Figure 2. Measurement system of Reflection coefficient based on free space method of reflection type.

h_{LC} . The unit cell reflection phase change is usually less than 360 degrees when a single patch structure is used and three dipole structure as Model A is used in references [3] and is capable of obtaining a phase change exceeding 360 degrees. However, the width of dipole w is narrow as the number of dipole increases and the quality factor of resonance (Q-value) will be high. As shown in Model B, the width can be increased within the constraints of pitch p of half wavelength, by decreasing the number of dipoles to two elements, making it possible to lower Q-value. The necessity of low Q-value will be discussed in Section IV.

III. MEASUREMENT OF REFLECTION COEFFICIENT

Figure 2 shows the measurement system of reflection coefficient of LC-IRS, generally called as the Free Space Method of reflection type [4]. A wideband antipodal fermi antenna [5] illuminates a dielectric lens focused on the surface of LC-IRS and the reflected wave was measured by a vector network analyzer (Keysight P5008A). The same voltage is applied for each element and the applied voltage V_{LC} is

changed from 0 V to 30 V by the multichannel voltage source with frequency of 100 kHz.

Figure 3 shows the voltage characteristics of reflection phase change $\Delta\Phi (= \phi(V_{LC}=V_{max}) - \phi(V_{LC}=0V))$ where V_{max} is the maximum voltage of $V_{max}=30$ V, and also shows reflection magnitude change at the frequencies of 47 GHz for Model A, and 47.8 GHz for Model B. Large amount of phase changes of over 360 degrees have been obtained for both Model A and Model B. The maximum phase change of 449 deg at 47 GHz and 432 deg at 48.2 GHz were obtained. Smooth phase changes were observed for both model as the voltage increases, however, magnitude changes were totally different. In case of Model A, the magnitude with large change from -21 dB to -6 dB was observed when voltage changes from 0 V to 10 V. On the other hand, relatively small change of magnitude was obtained in the case of Model B. Note that almost constant magnitude was obtained in a voltage range of 10 V to 20 V. These results show that low Q-value of resonance contributes to the small change of magnitude.

IV. ARRAY FACTOR ANALYSIS

Considering the scattered beam scanning with angle of $\theta_s=20$ deg by selecting the phases of each element #1~#15 in Figure 1 from phase change chart as a function of voltages shown in Figure 3. Figure 4 shows the reflection magnitude distributions when the scattering angle is $\theta_s=20$ deg. In case of Model A, strong magnitude variation was observed, on the other hand, almost uniform aperture distribution was observed in case of Model B. Figure 5 shows the array factor calculated by the complex reflection coefficient distribution shown in Figure 4. Low sidelobe level of -14 dB was obtained in case of Model B, on the other hand, high sidelobe level of -7 dB was observed in case of Model A, corresponding to the difference of aperture, reflection magnitude distributions.

V. CONCLUSION

In this paper, design of Liquid Crystal-based Intelligent Reflecting Surface at 47 GHz band has been presented. It is demonstrated that the structure of unit cell with wide width two dipoles contributes to the uniform reflection magnitude distribution result in a low sidelobe scattering pattern.

ACKNOWLEDGMENT

This research was partly supported by the Ministry of Internal Affairs and Communications in Japan (JPJ000254).

REFERENCES

- [1] X. Li, H. Sato, H. Fujikake and Q. Chen, "Development of Two-dimensional Steerable Reflectarray with Liquid Crystal for Reconfigurable Intelligent Surface Application," in IEEE Transactions on Antennas and Propagation, doi: 10.1109/TAP.2024.3354054.
- [2] X. Li, H. Sato, Y. Shibata, T. Ishinabe, H. Fujikake and Q. Chen, "Development of Beam Steerable Reflectarray with Liquid Crystal for Both E-Plane and H-Plane," in IEEE Access, vol. 10, pp. 26177-26185, 2022, doi: 10.1109/ACCESS.2022.3155544.
- [3] G. Perez-Palomino et. al., "Design and Demonstration of an Electronically Scanned Reflectarray Antenna at 100 GHz Using Multiresonant Cells Based on Liquid Crystals," in IEEE Transactions on Antennas and Propagation, vol. 63, no. 8, pp. 3722-3727, Aug. 2015, doi: 10.1109/TAP.2015.2434421.
- [4] L. Li, H. Hu, P. Tang, R. Li, B. Chen and Z. He, "Compact Dielectric Constant Characterization of Low-Loss Thin Dielectric Slabs With Microwave Reflection Measurement," in IEEE Antennas and Wireless Propagation Letters, vol. 17, no. 4, pp. 575-578, April 2018, doi: 10.1109/LAWP.2018.2803769.

- [5] H. Sato, Y. Takagi, and K. Sawaya, "High gain antipodal fermi antenna with low cross polarization," IEICE transactions on communications, vol. 94, no. 8, pp. 2292-2297, 2011.

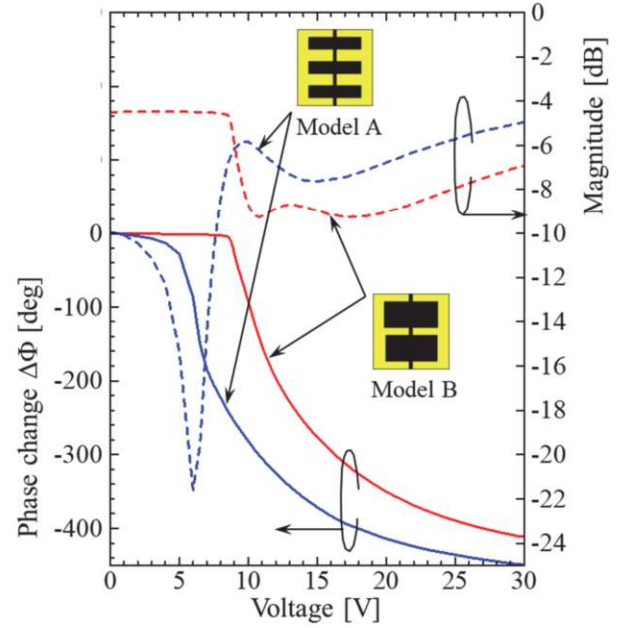


Figure 3. Frequency characteristics of phase change $\Delta\Phi$ and magnitude change. $\Delta\Phi = \phi(V_{LC}=V_{max}) - \phi(V_{LC}=0V)$, $V_{max}=30$ V

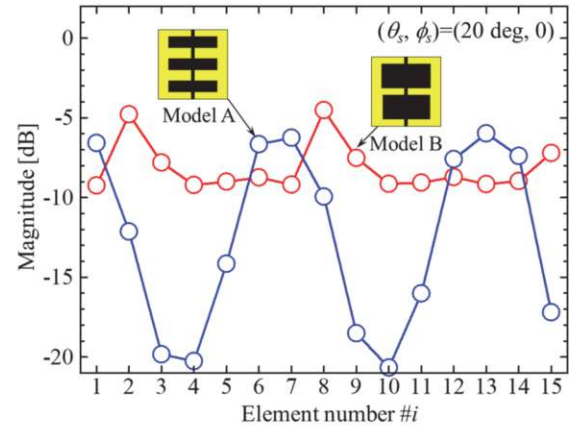


Figure 4. Reflection magnitude distributions when $\theta_s=20$ deg.

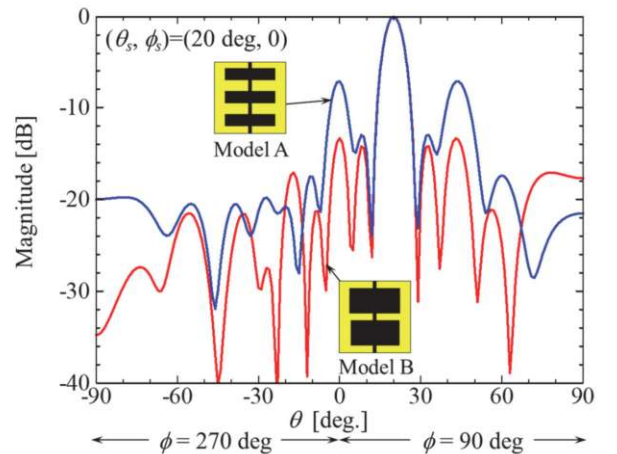


Figure 5. Array factor calculated using Figure 4.